International Journal of Engineering & Technology, 7 (4.14) (2018) 515-519

International Journal of Engineering & Technology

Website: www.sciencepubco.com/index.php/IJET

Research paper



Ion Transport Mechanism in Flexible $PMMA_{IL}$/LiTf Films

Nabilah Akemal Muhd Zailani[1], Famiza Abdul Latif [1]*, Ab Malik Marwan Ali [1,3,4], Mohd Azri Ab Rani [1], Muhd Zu Azhan Yahya [2,4]

[1]*Faculty of Applied Sciences, Universiti Teknologi MARA, 40450 Shah Alam, Selangor, Malaysia*
[2]*Faculty of Defence Science & Technology, Universiti Pertahanan Nasional Malaysia, 57000 Kuala Lumpur, Malaysia*
[3]*Institute of Science, Universiti Teknologi MARA, 40450 Shah Alam, Selangor, Malaysia*
[4]*Ionic Material & Devices (iMADE) Research Laboratory, Faculty of Applied Sciences, Universiti Teknologi MARA, 40450 Shah Alam, Selangor, Malaysia*
**Corresponding author E-mail: famiza@salam.uitm.edu.my*

Abstract

Acrylates such as poly (methyl methacrylate) (PMMA) has been widely studied as polymer electrolyte film due to its good mechanical stability towards lithium electrode. However, commercial PMMAs even at high molecular weight are not able to produce flexible films due to their polar nature that prone to form interchain crosslinking via hydrogen bonding. Therefore, the formation of hydrogen bonding was hindered by incarcerating ionic liquid (IL) of 1-methyl-3-pentamethyldisiloxymethylimidazolium bis(trifluoromethylsulfonyl)imide, [(SiOSi)C_1C_1im] [NTf_2] during free radical polymerization of MMA. Interestingly, the synthesized PMMA containing IL ($PMMA_{IL}$) produced flexible and free standing films with ionic conductivity of ~10^{-7} S cm^{-1}. Though the ionic conductivity obtained is comparable with other doped PMMA film electrolytes that had been studied, it is still considered as low for application in energy storage devices. As an alternative, in this study, lithium triflate (LiTf) salt was added into the $PMMA_{IL}$ system and the highest ionic conductivity obtained was 2.65 ×10^{-4} S cm^{-1} with addition of 30 wt.% LiTf at ambient temperature. The temperature dependence conductivity and AC conductivity behaviour of $PMMA_{IL}$/LiTf were further investigated in order to fully understand the ion transport mechanism that occurred in the system. It was found that the $PMMA_{IL}$/LiTf system fits the Arrhenius behaviour and Correlated Barrier Hopping (CBH) model.

Keywords: *Ionic liquid; ion transport mechanism; lithium triflate; PMMA; polymer electrolytes.*

1. Introduction

Nowadays, the development of polymer electrolyte is of high interest as it is considered as a safer choice if compared to liquid electrolyte that is susceptible to leakage and explosion [1]. PMMA is an acrylic glass that has been extensively studied as polymer electrolyte [2-4] due to its stability towards lithium electrode [5]. However, the stability towards lithium electrode could only be achieved when PMMA is fabricated in a thin film form. To date fabricating PMMA film is a challenge since commercial PMMAs produced brittle films [2] which poorly adhere to the electrode hence creating additional resistance for the ionic conduction. Several modifications have been made to improve the contact between the electrode and the electrolyte such as blending it with another polymer [2], adding plasticizers [3] or organic fillers [4], etc. However, these attempts were mostly unsuccessful due to poor mechanical properties caused by plasticizer, agglomeration due to the filler and poor homogeneity of the film when blended with other polymers. Recently, the addition of ionic liquids, (IL) such as 1-butyl-3-methylimidazolium bis(trifluoromethylsulfonyl) imide [6], 1-butyl-3-methylimidazolium tetrachloroferrate [7] etc. have slightly improved the brittleness of the film. However, the ionic conductivity achieved is still low, i.e. less than 10^{-4} S cm^{-1} which is below the minimal requirement for application in any energy storage devices. This is probably due to the polar nature of PMMA that is prone to form interchain crosslinking via hydrogen bonding. In our previous work, the formation of hydrogen bonding was hindered by incarcerating IL, [(SiOSi)C_1C_1im] [NTf_2] during free radical polymerization of MMA. The synthesized PMMA containing IL ($PMMA_{IL}$) produced flexible and free standing films with ionic conductivity of ~10^{-7} S cm^{-1} [8]. Though the ionic conductivity obtained is comparable with other doped PMMA film electrolytes that had been studied [9, 10], it is still considered as low for application in energy storage devices. Thus, in this study, the ionic conductivity of $PMMA_{IL}$ was further enhanced by addition of LiTf in order to provide the additional conducting species to the system. The ion transport mechanism of $PMMA_{IL}$/LiTf was also determined by investigating the temperature dependence conductivity and AC conductivity behaviour of the system.

2. Experimental

2.1. Synthesis of bulk $PMMA_{IL}$

The bulk $PMMA_{IL}$ was synthesized by incarceration of (SiOSi)C_1C_1im] [NTf_2] during free radical polymerization of MMA as previously reported [8].

2.2. Preparation of Film

The bulk $PMMA_{IL}$ was then made into films by solvent casting technique [9]. The $PMMA_{IL}$ with wt.% composition of MMA: [(SiOSi)C_1C_1im] [NTf_2] (70:30) was chosen to be doped with LiTf due to its high ionic conductivity and amorphosity if compared to the other compositions [8]. To obtain the salt doped $PMMA_{IL}$ films, the solution casting technique was applied using fixed

Copyright © 2018 Authors. This is an open access article distributed under the Creative Commons Attribution License, which permits unrestricted use, distribution, and reproduction in any medium, provided the original work is properly cited.

amount of bulk $PMMA_{IL}$ (0.3 g) and varied amount of salt (0-50 wt.% LiTf). This system was then denoted as D*x*-$PMMA_{IL}$ system.

2.3. Characterization Techniques

The impedance measurement of the film samples was obtained using HIOKI 3532-50 LCR Hi Tester analyzer in the frequency range of 100 Hz to 1 MHz at 303K-318 K. From the impedance plots obtained, the bulk resistance (R_b) of each sample was determined and the ionic conductivity (σ) of the samples were calculated using equation (1) [11]:

$$\sigma = \frac{l}{R_b \cdot A} \tag{1}$$

where R_b is the bulk resistance (Ω), l is the sample thickness (cm) and A is the effective contact area of the electrode and the electrolyte (cm^2). From the impedance data, the dielectric constant (ε_r), dielectric loss (ε_i), real part of electrical modulus (M_r) and imaginary electric modulus (M_i) were obtained from the following equations [11].

$$\varepsilon_r = \frac{Z_i}{\omega \cdot C_0 (Z_r^{\,2} + Z_i^{\,2})} \tag{2}$$

$$\varepsilon_i = \frac{Z_r}{\omega \cdot C_0 (Z_r^{\,2} + Z_i^{\,2})} \tag{3}$$

$$M_r = \frac{\varepsilon_r}{(\varepsilon_r + \varepsilon_i)} \tag{4}$$

$$M_i = \frac{\varepsilon_i}{(\varepsilon_r + \varepsilon_i)} \tag{5}$$

where C_0 is equal to $\varepsilon_0 A/t$, ε_0 is the permittivity of the free space (8.85×10^{-14} F cm^{-1}) and ω is angular frequency ($\omega = 2\pi f$).

3. Results and Discussion

3.1 Formation of Films

Solid, transparent, flexible and free standing films were obtained when 5, 10, 20, 30 and 40 wt% of LiTf were added into the $PMMA_{IL}$ system (Figure 1). However, the addition of > 40 wt% of LiTf produced sticky film, thus the sample was discarded and not further characterised.

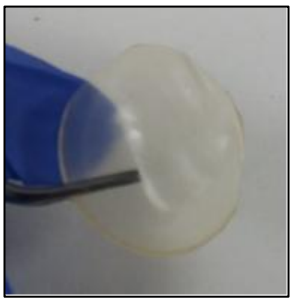

Fig. 1: D30-$PMMA_{IL}$ Film

3.2 Conductivity Studies for D*x*-$PMMA_{IL}$ System

Figure 2 illustrates the variation of ionic conductivity for D*x*-$PMMA_{IL}$ system with different wt% of LiTf at room temperature. The ionic conductivity is observed to increase with increasing LiTf content up to 30 wt% and then decreases when 40 wt% of LiTf was added. Maximum ionic conductivity of 2.65×10^{-4} S cm^{-1} was achieved when 30 wt% of LiTf was added into the system. Thus, it can be concluded that the incorporation of LiTf had successfully enhanced the ionic conductivity of $PMMA_{IL}$ up to three order of magnitude from ~10^{-7} S cm^{-1} [8] to ~10^{-4} S cm^{-1}.

The ionic conductivity of polymer electrolyte system can be ascribed as equation below [12]:

$$\sigma = \sum nq\mu \tag{6}$$

where n is the number of charge carriers, q refers to the charge and μ is the mobility of the charge carriers. Thus, it can be explained that the rise in the ionic conductivity is due to the increase in number of charge carrier as the salt content increases. The addition of >30 wt% of LiTf however leads to a drop in ionic conductivity and this can be due to the formation of ion pairs or ion aggregates which reduce the number of charge carriers [13].

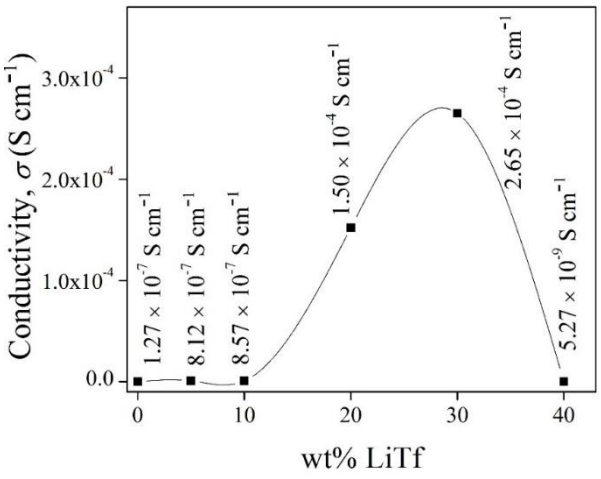

Fig. 2: Conductivity versus wt% of LiTf for D*x*-$PMMA_{IL}$ system

In order to analyse the mechanism of ionic conduction, the ionic conductivity of the D*x*-$PMMA_{IL}$ system was obtained at different temperatures starting from 303K to 318K (Table 1). The graph of log σ versus 1000/T for Dx-$PMMA_{IL}$ system is illustrated in Figure 3. The graph shows linear plots with the regression values close to unity (~0.99) indicating that the plots obey Arrhenius rule in which the ionic conduction in these materials is thermally assisted and can be expressed as in equation (7):

$$\sigma = \sigma_0 \exp\left(\frac{E_a}{K_B T}\right) \tag{7}$$

where σ_0 is the pre-exponential factor, E_a is the activation energy, K_B is the Boltzmann constant, and T is the absolute temperature.

As the plots follow Arrhenius behaviour, the nature of cation transport in this system is quite similar to that in ionic crystals which use the ion hopping mechanism [14]. Thus, it is suggested that the increase in the conductivity with temperature might be due to these two factors; (i) the presence of kinetic effect as temperature increase which helps to assist the transportation of ions via ion hopping and also helps to increase the dissociation of salt [11], (ii) the increase of the temperature causes the expansion of the polymer hence providing more free volume which makes it easier for the ions to hop [15]. The E_a can be defined as the energy required for the ions to successfully hop from one complexation site to another. The E_a for each sample is determined from the slope of the log σ versus 1000/T and the values obtained are listed in Table 1. It was observed that the highest ionic conducting sample (D30-$PMMA_{IL}$) exhibits the lowest values of E_a indicating that less energy is required for ion transportation.

Table 1: The σ and E_a for D*x*-PMMA$_{IL}$ System

System	Ionic conductivity, σ (10^{-4} S cm^{-1})				E_a (eV)
	303 K	308 K	313 K	318 K	
D5-PMMA$_{IL3}$	0.008	0.013	0.021	0.033	0.79
D10-PMMA$_{IL3}$	0.008	0.014	0.022	0.033	0.74
D20-PMMA$_{IL3}$	1.50	2.14	2.90	3.90	0.53
D30-PMMA$_{IL3}$	2.65	3.20	3.60	4.10	0.24
D40-PMMA$_{IL3}$	0.00005	0.00008	0.00013	0.00029	0.95

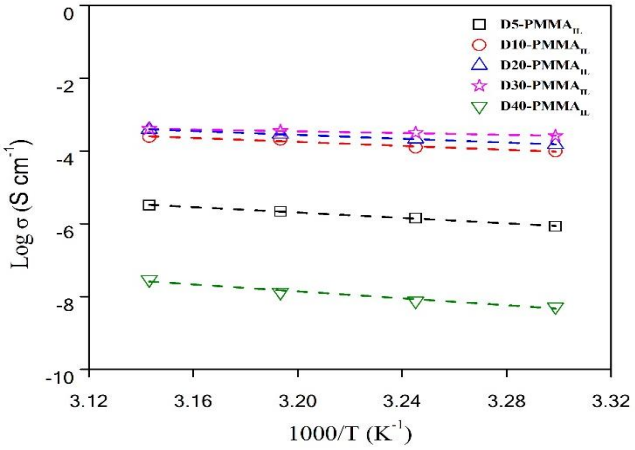

Fig. 3: Log σ versus 1000/T for D*x*-PMMA$_{IL}$ System

3.2. Dielectric Studies for D30-PMMA$_{IL}$

The dielectric properties for the highest conducting sample (D30-PMMA$_{IL}$) at different temperature was further studied. The dielectric constant (ε_r) can be defined as the measure of the stored electric charges while dielectric loss (ε_i) is the measure of the energy loses to align the charges in every cycle of the applied electric field [16]. The ε_r and ε_i versus log *f* are shown in Figure 4. The rise of ε_r and ε_i at low frequency indicate that the phenomenon of the electrode polarization has occurred as the charges have enough time to accumulate at the electrode-electrolyte interface before the electric field changes the direction. The reversal rate of the electric field increase at high frequency and this provides no time for the charges to accumulate at the interface resulting in low ε_r and ε_i [16]. It was observed that there is only slight increase of the ε_r and ε_i values with each increment of the temperature which means that there is no significant difference in the number of charges present. Thus, it can be concluded that the increase in temperature did not help in dissociation of salt and the increase in conductivity however is probably due to high temperature which assist in the ion transportation and polymer expansion.

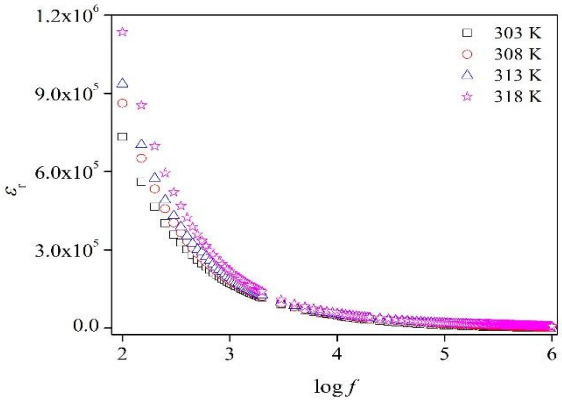

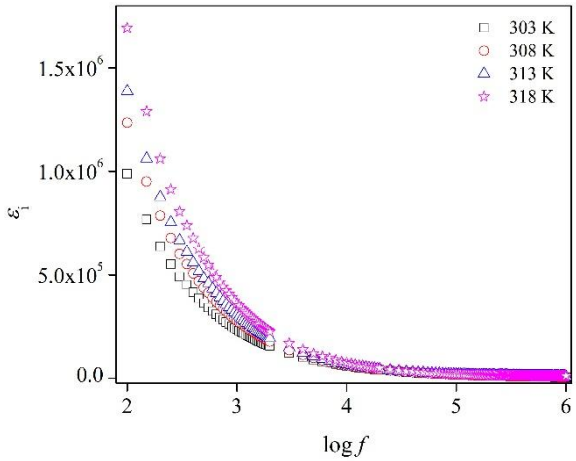

Fig. 4: (a) ε_r versus log *f* and (b) ε_r versus log *f* for D30-PMMA$_{IL}$ at Different Temperatures

The real (M_r) and imaginary (M_i) part of electrical modulus represent the reciprocal of ε_r and ε_i respectively [11]. The variation of M_r and M_i versus log *f* are shown in Figure 5. At low frequencies region, M_r and M_i values tend to zero signifying that electrode polarization phenomena were almost negligible. There was no peak observed in the M_r and M_i plots indicating the absence of the relaxation peak as the ions are mobile over a long distances.

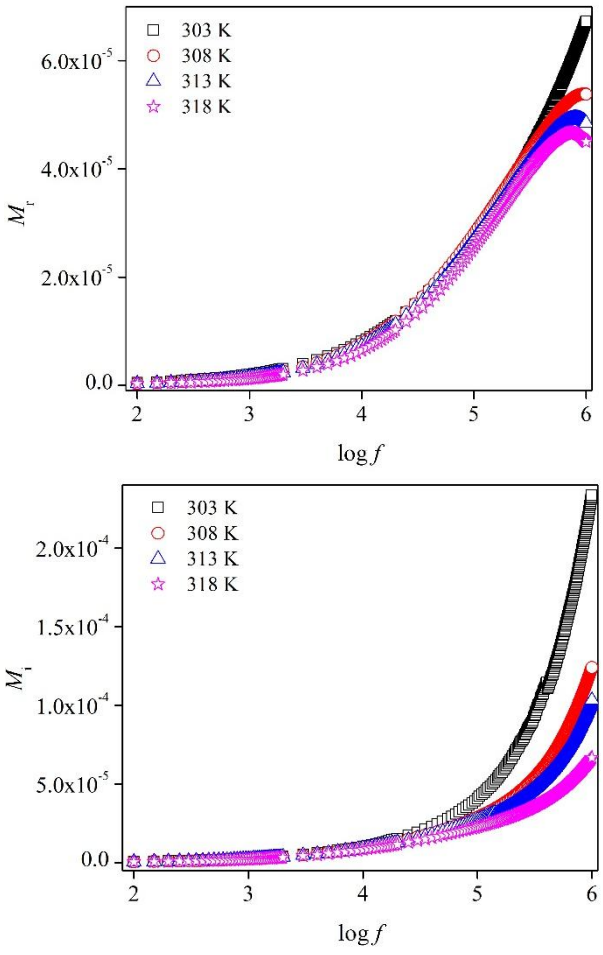

Fig. 5: (a) M_r versus log *f* and (b) M_i versus log *f* for D30-PMMA$_{IL}$ at Different Temperature

3.2. AC Conductivity Studies for D30-PMMA$_{IL}$

The AC conductivity (σ_{ac}) studies for the highest conducting sample (D30-PMMA$_{IL}$) was done in order to further understand the

ion hopping mechanism occurred in the sample. The values of σ_{ac} was calculated according to the equation (8) below [11].

$$\sigma_{ac} = \varepsilon_0 \omega \varepsilon_i \tag{8}$$

where ε_0 is the permittivity of the free space, ε_i is the dielectric loss and ω is angular frequency. In general, the AC conductivity can be analyzed using Jonscher's universal power law [17].

$$\sigma_{ac}(\omega) = \sigma_{dc} + A\omega^s \tag{9}$$

where the σ_{dc} is the frequency-independent DC conductivity, A is a parameter dependent on temperature, ω is the angular frequency and s is the power law exponent which range in between 0 and 1. The plot of σ_{ac} versus log f at different temperature for D30-PMMA$_{IL}$ is shown in Figure 6. It was observed that the plot exhibits two distinct regions which consists of the almost plateau region at low frequency and dispersive region at high frequency; representing DC conductivity (σ_{dc}) and AC conductivity (σ_{ac}) respectively. The value of σ_{dc} can be obtained by extrapolating the plateau region to zero frequency and the values were in agreement with that calculated based on the impedance plots.

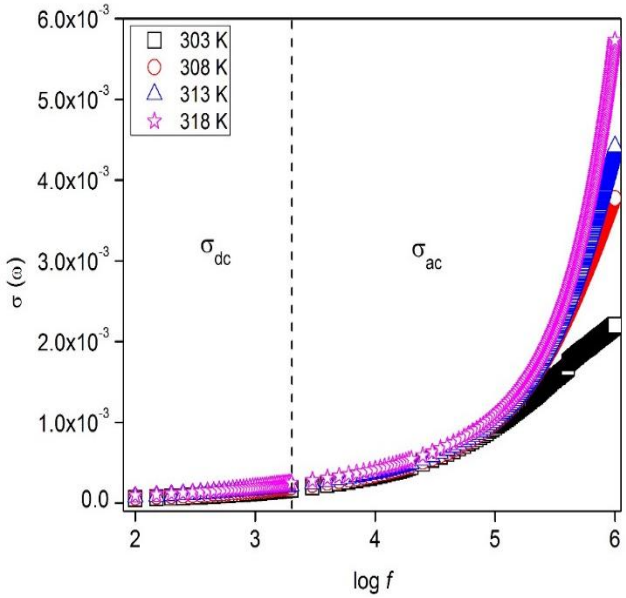

Fig. 6: σ(ω) versus log f for D30-PMMA$_{IL}$

By referring to Jonscher's universal power law, the conductivity dispersion region was represented by σ_{ac} and can be expressed as:

$$\sigma_{ac} = A\omega^s \tag{10}$$

There are a few models which relate the temperature dependence of exponent s with the conduction mechanism of the materials. To obtain the values of s, equation (11) was derived based on equation (9) and equation (10):

$$\ln \varepsilon_i = \ln \frac{A}{\varepsilon_0} + (s-1)\ln \omega \tag{11}$$

The graph of ln ε_i versus ln ω is plotted according to equation (11) and shown in Figure 7. In this study, the acceptable frequency range for ln ω is chosen from 8 to 12 as these region shows minimal electrode polarisation effect [18].

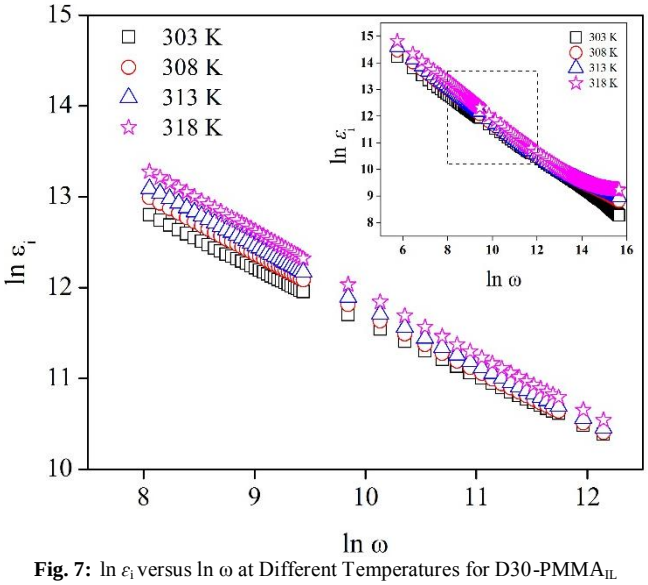

Fig. 7: ln ε_i versus ln ω at Different Temperatures for D30-PMMA$_{IL}$

Then, the values of exponent s were obtained from the slope of the ln ε_i versus ln ω graph. The variation of s with temperature is shown in Figure 8. The values obtained for s exponent is in between 0.32-0.40 as the temperature varies from 303K to 318 K. The behaviour of s is in agreement with the correlated barrier hopping model (CBH) [19] as the s exponent decreases with increasing temperature. Thus, it can be said that the ionic conduction occurs through the hopping process of Li^+ ions of the salt over the potential barrier, suggestively due to the bulky structure of [(SiOSi)C_1C_1im][NTf_2] that exists between the two complexation sites.

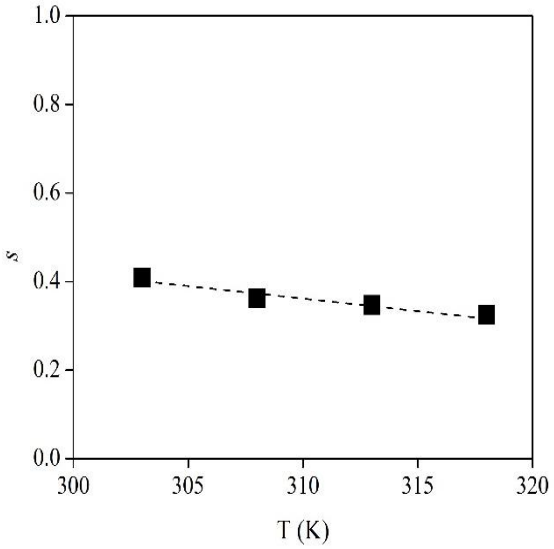

Fig. 8: s versus T for D30-PMMA$_{IL}$

For CBH model, the exponent s can be expressed as [20]:

$$s = 1 - \frac{6K_BT}{W_M} \tag{12}$$

where K_B is the Boltzmann constant (8.62×10^{-5} eV.K^{-1}), T is the temperature in Kelvin and W_M is the binding energy or the energy required to move an ion from one complexion site to another one [19]. The values of W_M are calculated based on equation (12) and the plot of W_M versus T is shown in Figure 9.

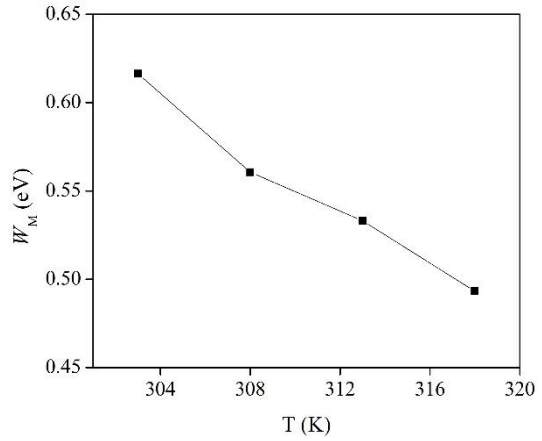

Fig. 9: *s* versus T for D30-$PMMA_{IL}$

It was observed that the values of W_M decreases with increasing temperature. This means that, it is easier for the free ions to jump over the barrier and bind from one complexation site to another as temperature increase. This can be related to the kinetic effect and expansion of the polymer which help in the transportation of ions as temperature increase [11, 15].

The power law of exponent *s* also can be used to predict the tendency of charge carrier to back hop or relax as s is equal to ratio of initial backhop rate to initial site relaxation rate [21]. Thus, in this study, as $s < 1$, the possibility for the ion to relax at the new site is greater than the possibility to jump back to its initial site and this proves the successful of the 'initial forward' hop in this system.

4. Conclusion

A flexible film with enhanced ionic conductivity up to 3 order of magnitude from ~10^{-7} S cm^{-1} to ~10^{-4} S cm^{-1} was successfully obtained when 30 wt% of LiTf was added into the $PMMA_{IL}$ (D30-$PMMA_{IL}$). It can be also be concluded that the D*x*-$PMMA_{IL}$ system follows the Arrhenius behaviour in which the ionic conduction occurs through the ion hopping mechanism. Further investigation on the AC conductivity of D30-$PMMA_{IL}$ reveals that it is in agreement with the CBH model, which indicates that the Li^+ ions need to jump over the potential barrier arises from the bulky structure of ionic liquid, [(SiOSi)C_1C_1im][NTf_2] in order to move from one complexation site to another.

Acknowledgement

The authors would like to express their thankfulness to the Faculty of Applied Sciences, UiTM, i-MADE Lab, ICC Lab and Institute of Science for their support in providing research facilities. Financial supports from Malaysia Toray Science Foundation (MTSF) (Ref: TMLC-CA/13.206 [File Ref: 16/G236]), Bestari Perdana grant (Ref. No: 600-IRMI/PERDANA 5/3 BESTARI (083/2018)) and MyBrain SC scholarship are highly acknowledged.

References

[1] Agrawal, R. C., & Pandey, G. P. (2008). Solid polymer electrolytes: materials designing and all-solid-state battery applications: an overview. Journal of Physics D: Applied Physics, 41(22), 223001.

[2] Latif, F.A. (2006). Preparation and characterization of poly (methyl methacrylate)/50% epoxidised natural rubber based solid electrolytes for lithium-ion secondary battery (Doctoral dissertation, Universiti Teknologi Malaysia).

[3] Rajendran, S., Sivakumar, M., & Subadevi, R. (2004). Investigations on the effect of various plasticizers in PVA–PMMA solid polymer blend electrolytes. Materials Letters, 58(5), 641-649.

[4] Chew, K. W., & Tan, K. W. (2011). The effects of ceramic fillers on PMMA-based polymer electrolyte salted with lithium triflate, $LiCF_3SO_3$. International Journal of Electrochemical Science, 6, 5792-5801.

[5] Appetecchi, G. B., Croce, F., & Scrosati, B. (1995). Kinetics and stability of the lithium electrode in poly(methylmethacrylate)-based gel electrolytes. Electrochimica Acta, 40(8), 991-997.

[6] Xie, Z. L., Xu, H. B., Geßner, A., Kumke, M. U., Priebe, M., Fromm, K. M., & Taubert, A. (2012). A Transparent, flexible, ion conductive, and luminescent PMMA ionogel based on a Pt/Eu bimetallic complex and the ionic liquid [Bmim][$N(Tf)_2$]. Journal of Materials Chemistry, 22(16), 8110-8116.

[7] Xie, Z. L., Jeličić, A., Wang, F. P., Rabu, P., Friedrich, A., Beuermann, S., & Taubert, A. (2010). Transparent, flexible, and paramagnetic ionogels based on PMMA and the iron-based ionic liquid 1-butyl-3-methylimidazolium tetrachloroferrate (III) [Bmim][$FeCl_4$]. Journal of Materials Chemistry, 20(42), 9543-9549.

[8] Zailani, N. A. M., Latif, F. A., Ali, A. M. M., Zainuddin, L. W., Kamaruddin, R., & Yahya, M. Z. A. (2017). Effect of ionic liquid incarceration during free radical polymerization of PMMA on its structural and electrical properties. Ionics, 23(2), 295-301.

[9] Azuan, M., Husna, S. I., Abdul Latif, F., Zamri, M., & Fadli, S. (2016). Effects of dodecanoic acid modified SiO_2 on filler dispersion and ionic conductivity of PMMA/ENR-50/$LIBF_4$ Electrolytes. Materials Science Forum, 846, 528-533.

[10] Shukla, N., & Thakur, A. K. (2009). Role of salt concentration on conductivity optimization and structural phase separation in a solid polymer electrolyte based on PMMA-$LiClO_4$. Ionics, 15(3), 357–367.

[11] Muhammad, F. H., Jamal, A., & Winie, T. (2016). Dielectric and AC conductivity behavior of hexanoyl chitosan-NaI based polymer electrolytes. International Journal of Advanced and Applied Sciences, 3(10), 9-13.

[12] Ratner, M. A., & Shriver, D. F. (1988). Ion Transport in Solvent-Free Polymers. Chemical Reviews, 88, 109–12.

[13] Kadir, M. F. Z., Majid, S. R., & Arof, A. K. (2010). Plasticized chitosan - PVA blend polymer electrolyte based proton battery. Electrochimica Acta, 55(3), 1475–1482

[14] Ramesh, S., & Chai, M. F. (2007). Conductivity, dielectric behavior and FTIR Studies of high molecular weight poly(vinylchloride)–lithium triflate polymer electrolytes. Materials Science and Engineering: B, 139(2–3), 240–245.

[15] Jamal, A., Muhammad, F. H., Ali, A. M. M., & Winie, T. (2017). Blends of hexanoyl chitosan/epoxidized natural rubber doped with EMImTFSI. Ionics, 23(2), 357-366.

[16] Abidin, S. Z. Z., Yahya, M. Z. A., Hassan, O. H., & Ali, A. M. M. (2014). Conduction mechanism of lithium bis(oxalato)borate – cellulose acetate polymer gel electrolytes. Ionics, 20(12), 1671–1680.

[17] Jonscher, A. K. (1977). The universal dielectric response. Nature, 267(5613), 673–679.

[18] Buraidah, M. H., Teo, L. P., Majid, S. R., & Arof, A. K. (2009). Ionic conductivity by correlated barrier hopping in NH_4I doped chitosan solid electrolyte. Physica B: Condensed Matter, 404(8-11), 1373-1379.

[19] Taher, Y. Ben, Maaloul, A. O. N. K., & Gargouri, K. K. M. (2015). Conductivity study and correlated barrier hopping (CBH) conduction mechanism in diphosphate compound. Applied Physics A: Materials Science and Processing, 120, 1537–1543.

[20] Mahmoud, K. H., Abdel-Rahim, F. M., Atef, K., & Saddeek, Y. B. (2011). Dielectric dispersion in lithium–bismuth-borate glasses. Current Applied Physics, 11(1), 55-60.

[21] Funke, K. (1997). Ion Transport in Fast Ion Conductors. Solid State Ionics, 94, 27–33.